Conformational studies of membrane-associated antimicrobial peptide diptericin in bicellar environment using solution state NMR

Agrim Gupta

A dissertation submitted for the partial fulfilment
of BS-MS dual degree in Science

Indian Institute of Science Education and Research Mohali
April 2018

Certificate of Examination

This is to certify that the dissertation titled **Conformational studies of membrane-associated antimicrobial peptide diptericin in bicellar environment using solution state NMR** submitted by **Agrim Gupta** (Reg. No. MS13006) for the partial fulfillment of BS-MS dual degree programme of the Institute, has been examined by the thesis committee duly appointed by the Institute. The committee finds the work done by the candidate satisfactory and recommends that the report be accepted.

Dr. Sandeep Kumar Goyal Dr. Samir Kumar Biswas Dr. Kavita Dorai
(Supervisor)

Dated: April 20, 2018

Declaration

The work presented in this dissertation has been carried out by me under the guidance of Dr. Kavita Dorai at the Indian Institute of Science Education and Research Mohali.

This work has not been submitted in part or in full for a degree, a diploma, or a fellowship to any other university or institute. Whenever contributions of others are involved, every effort is made to indicate this clearly, with due acknowledgement of collaborative research and discussions. This thesis is a bonafide record of original work done by me and all sources listed within have been detailed in the bibliography.

Agrim Gupta
(Candidate)

Dated: April 20, 2018

In my capacity as the supervisor of the candidates project work, I certify that the above statements by the candidate are true to the best of my knowledge.

Dr. Kavita DOrai
(Supervisor)

Acknowledgment

Firstly I would like to express my deepest gratitude to my advisor Dr. Kavita Dorai for giving me chance to explore the field of NMR. This project would not have been possible without the guidance and support provided by her. I would like to thank my thesis committee, Dr. Kavita Dorai (Supervisor) , Dr. Sandeep K. Goyal and Dr. Samir Kumar Biswas for taking out the time to read my thesis and giving valuable suggestions. I would also like to thank IISER Mohali for giving me this wonderful opportunity to study in a research-oriented environment.

I would also like to thank Jyotsana Ojha and Navdeep Gogna for helpful suggestions and discussion throughout the project. I am thankful to my lab members for being supportive.

My sincere thanks to all of my friends for the wonderful memories at IISER. I also want to acknowledge Blood Donation Camp organizing team for helping me in organizing camps.

I would like to thank my parents and sister for always being there for me and encouraging me to face all sorts of difficulties I had. Without their constant support, I would not have gotten this far.

List of Figures

Notation

^1H	Proton
^{13}C	Carbon-13
δ	Chemical Shift
τ_c	Correlation time
NOE	Nuclear Overhauser Effect
COSY	Correlation Spectroscopy
TOCSY	Total Correlation Spectroscopy
HSQC	Heteronuclear Single Quantum Correlation
HMQC	Heteronuclear Multiple Quantum Correlation
HMBC	Heteronuclear Multiple Bond Correlation
NOESY	Nucleat Overhauser Effect Spectroscopy
ROESY	Rotational nuclear Overhauser Effect Spectroscopy
DMPC	1,2-dimyristoylphosphatidylcholine
DHPC	1,2-dihexanoylphosphatidylcholine
DMPG	dimyristoylphosphatidylglycerol
DMPS	dimyristoylphosphatidylserine
DMPE	dimyristoylphosphatidylethanolamine

Abstract

Antimicrobial peptides (AMPs) are an important component of natural defense of all life forms against invading pathogens. The target of these peptides is the microbial membrane and there are numerous models to explain their mechanism of action ranging from pore formation to general membrane disruption. We here are studying the conformational studies of diptericin, an 82 residue glycopeptide. It is the key AMP of Drosophilas innate immunity and is active only against gram negative bacteria. It also inhibits the outer membrane protein synthesis. To study the conformational change of the peptide on association with bacterial membrane, identical membrane mimic is required. SDS micelles are used as a membrane mimic earlier, but to get ideal membrane environment, it has been replaced with bicelles which are bilayer lipid micelles. The peptide-bicelle association can be studied by 2D COSY, NOESY, TOCSY, ROESY, HSQC, HMBC spectra and the NMR peak assignment followed by structure prediction software which give us the validation and information about the structure of the protein.

Contents

Chapter 1

Introduction

1.1 NMR Phenomenon

NMR stands for Nuclear Magnetic Resonance. NMR spectroscopy is an eminent technique used in quality control and research to determine the molecular structure of unknown organic compounds. Once the basic structure is known, it can be used to determine molecular conformation in solution as well as studying physical properties at the molecular level such as conformational exchange , phase changes, solubility, and diffusion. Nowadays, it is prominent spectroscopic method amongst all because with just set of experiments, a detailed analysis can be done on the entire structure of compound.

It is the physical phenomenon based on the fact that when a population of magnetic nuclei with an odd mass number or an odd atomic number having nuclear spins, is placed in an external field, the nuclei become aligned in a predictable and finite number of orientations. It may be parallel or anti-parallel to the external magnetic field. In NMR, electromagnetic radiation is used to flip the alignment of nuclear spins from low energy spin aligned state to high energy spin opposed state. The signal in this consists of radio frequency waves with frequencies equal to the energy gap between the spin states. The signal then recorded in terms of FID(Free Induction Decay) and then processed with Fourier transformations in order to get NMR spectrum [1]

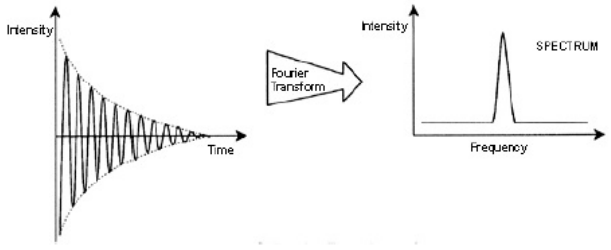

Figure 1.1: Fourier transformation of FID into the spectrum. Source: Bruker Biospin

1.2 Larmor Frequency

The nucleus has a positive charge and is spinning. This generates a small magnetic field. The nucleus therefore possesses a magnetic moment, m, which is proportional to its spin, I. [2]

$$\mu = \gamma I \hbar \tag{1.1}$$

The constant γ is called the gyromagnetic ratio which determines the resonant frequency of a nucleus when an external field is applied and is a fundamental nuclear constant which has a different value for every nucleus and h is Plancks constant. When as spin $\frac{1}{2}$ nucleus interacts with the magnetic field it gives rise to two energy levels α and β which is characterized by azimuthal quantum number m = $\frac{1}{2}$ (spin up) and m = $\frac{1}{2}$ (spin down). The interaction energy of a magnetic moment in a magnetic field B is

$$E = -\mu \cdot B_0 \tag{1.2}$$

Therefore,

$$E = -\gamma I \hbar B_0 \tag{1.3}$$

For a spin up level, energy ($E_\alpha = -\frac{\hbar}{2}\gamma B_0$) and for spin down level ($E_\beta = \frac{\hbar}{2}\gamma B_0$). The energy difference between two levels, α and β

$$\Delta E = \gamma \hbar B_0 \tag{1.4}$$

From Planck's law

$$\Delta E = hv \tag{1.5}$$

which implies

$$v = \frac{\gamma B_0}{2\pi} \tag{1.6}$$

or

$$\omega = \gamma B_0 \tag{1.7}$$

where ω is the Larmor frequency of the molecule. Larmor frequency is the frequency at which angular momentum vector of the nucleus precesses about the axis of the applied magnetic field. [3] Therefore energy associated with a spin flip can be written as

$$\Delta E = \hbar \omega \tag{1.8}$$

1.3 Relaxation

The tendency of an excited magnetization to return back to its equilibrium state is known as relaxation. NMR relaxation is used to study spectral assignment and also to study quadrupolar and paramagnetic interactions. Bloch theorem assumes that the equilibrium will be approached exponentially.The magnetization will decay according to:

$$\frac{dM_z}{dt} = \frac{M_o - M_z}{T_1} \tag{1.9}$$

$$\frac{dM_x}{dt} = \frac{-M_x}{T_2} \tag{1.10}$$

$$\frac{dM_y}{dt} = \frac{-M_y}{T_2} \tag{1.11}$$

where M_o is the magnetization at equilibrium state, and M_x, M_y, M_z are magnetizations along x, y, z direction respectively. $T_1 and T_2$ are relaxation times. [10]

There are two types of relaxation, Spin-Lattice (T_1, also known as longitudinal relaxation, or relaxation in the z-direction) and Spin-Spin (T_2, also known as transverse relaxation, or relaxation in the x-y plane)

1.3.1 Longitudinal Relaxation T_1

The recovery of the nuclear spin magnetization along the z-axis towards its equilibrium value M_z is called longitudinal relaxation. In general,

$$M_z = M_o(1 - e^{-\frac{t}{T_1}}) \tag{1.12}$$

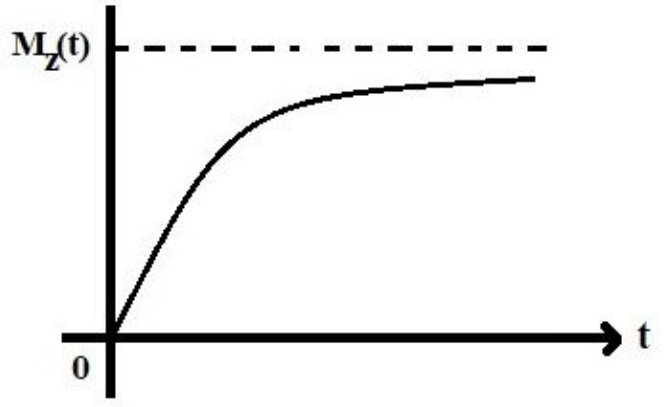

Figure 1.2: T_1 relaxation

1.3.2 Transverse relaxation T_2

T2 relaxation involves in the energy transfer between the interacting spins via the dipole-dipole and exchange interactions. It is used to quantify the rate of the decay of the magnetization within the x-y plane. After applying a 90^0 pulse, the nuclear spins will be aligned in one direction which we can say that it is because they are phase coherent. This mechanism is independent of the temperature. In general, T_2 value is always greater than T_1 value. The transverse magnetization will decay as,

$$M_{xy}(t) = M_{xy}(0)e^{-\frac{t}{T_2}} \tag{1.13}$$

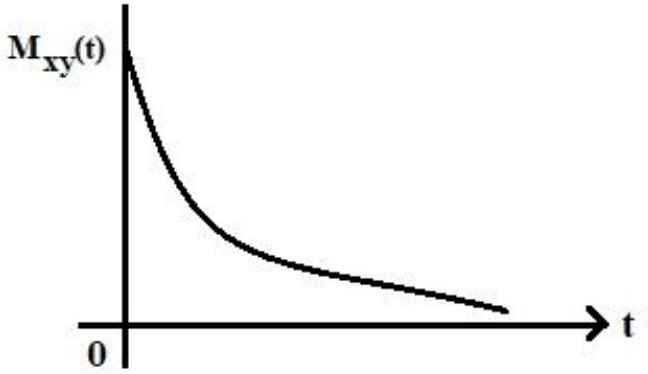

Figure 1.3: T_2 relaxation

1.4 Chemical Shift

The resonant frequency of the energy transition is linearly dependent on the strength of magnetic field at the nucleus. This field is affected by electron shielding which is in turn dependent on the chemical environment. As a result, information about the nucleus chemical environment can be derived from its resonant frequency. That's why it will appear at different positions according to the spectrometer frequency. In general, more electronegative the nucleus is, more is its resonant frequency. Other factors like magnetic anisotropy and hydrogen bonding affect the frequency shift. TMS (tetramethylsilane) is used as a proton reference frequency.This is because the precise resonant frequency shift of each nucleus depends on the magnetic field used. The chemical shift in ppm is given by

$$\delta = \frac{\omega - \omega_{ref}}{\omega_{ref}} * 10^6 \tag{1.14}$$

ω is the Larmor frequency of the nuclei and ω_{ref} is the Larmor frequency of reference compound i.e. TMS.

1.5 Spin-Spin coupling

The effective magnetic field is also affected by the orientations of the neighboring nuclei. The above effect is known as spin-spin coupling which can split the signal for each type of nucleus into two or more lines. The splitting pattern of a given nucleus (or set of equivalent nuclei) can be predicted by the n+1 rule, where n is the number of neighboring spin-coupled nuclei with the same. [2, 3]

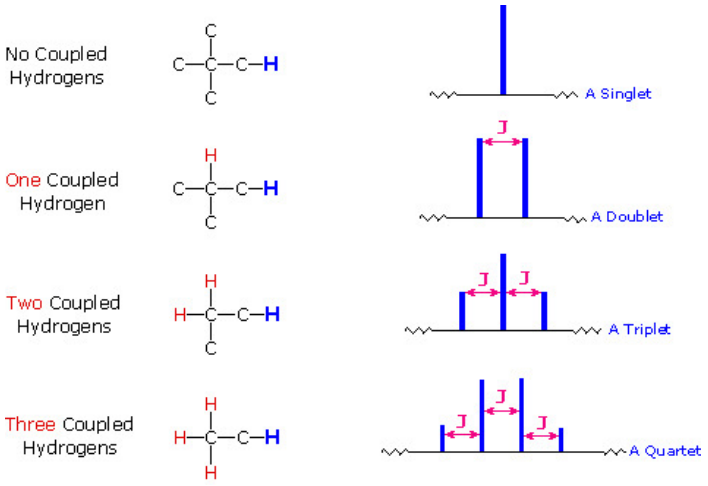

Figure 1.4: Splitting pattern of the nucleus. Source: MSU.edu

The size of the splitting called as coupling constant or J is interdependent of the magnetic field and is measured as an absolute frequency (in Hertz). The number of splittings indicates the number of chemically bonded nuclei in the vicinity of the observed nucleus.

1.6 Antimicrobial peptide

Antimicrobial peptides (AMPs) are an important component of self-defense against invading pathogens. The interaction between AMPs and target membrane is critical to the specificity and activity of these peptides. AMPs are used by organisms to combat microbial infections and effective in surviving the slow process of evolution. The AMPs exists in a wide range of secondary structures such as -helices, -strands with one or more disulphide bridges, loop and extended structures. This structural diversity of AMPs gives them a broad range of antimicrobial activity. Besides these properties, certain important factors are also responsible for their broad spectrum antimicrobial activity such as size, charge, hydrophobicity, amphipathic stereo geometry, and peptide association with the biological membrane. The

smaller size of AMPs facilitates secretion of peptide outside the cells, which is required for immediate defense response against pathogenic microbes. The antimicrobial specificity of AMPs towards the target cells was highly dependent on the preferential interaction of peptides with the microbial cells, which enable them to kill specific target cells without affecting the host cells. In addition, net charge and hydrophobicity of AMPs play a crucial role in the cellular association of these peptides to selective target cellular membranes in exerting antimicrobial activity. Most of them are cationic peptides, and only a few of them are anionic. Besides antimicrobial function, AMPs also serve as drug delivery vectors, anti-tumor agents, mitogenic agents, and signaling molecules in signal transduction pathways. [4, 5]

1.6.1 Diptericin

AMP here to be concerned is about diptericin. It is the key AMP of Drosophila's innate immunity. It consists of 82 amino acids and is rich in glycine residues. The sequence contains (DEKPKLILPTPAPPNLPQLVG^{21}GGGGNRKDGFGVSVDAHQKVWTSD^{45}NGRHSIGVT^{54} PGYSQHLGGPYGNSRPDYRIGAGYSYNF^{82}). This peptide is active only against gram-negative bacteria and it also inhibits the protein synthesis of the outer membrane, thus it increases the permeability of the outer membrane. [6] The peptide here is secreted from Drosophila's epithelial cell in response to its septic injury. [7]

Now we have to study the interaction of the peptide with the membrane of a cell, for that ideal membrane mimic is required. SDS micelles were used as a membrane mimic earlier but it is not accurate as membranes are bi-layered, so to get ideal membrane environment it has been replaced with bicelles which are bilayer lipid micelles.

1.7 Bicelle

Bicelles are an attractive membrane mimetic system because of their planar surface and lipid composition, which resemble biological membranes. Their orientation and morphologic properties make them useful for studying the interaction and structure of membrane peptides and proteins by solid- and solution-state NMR. Bicelles are made up of dimyristoylphosphatidylcholine (DMPC) and dihexanoylphosphatidylcholine (DHPC). The long chain lipid forms the planner region and the short chain lipid seals the rim region of the bicelle. Bicelle size is controlled both by the ratio of long-chain:short-chain phospholipid (q) and the total phospholipid concentration (cL). To mimic the diversity of biological membranes in a better way, the bicelle composition was also modified by incorporation of phospholipids with different polar headgroups. Negatively charged bicelles could be formed by substituting up to 25 mol% of DMPC by dimyristoylphosphatidylglycerol (DMPG) or dimyristoylphosphatidylserine (DMPS). PS is found in the membrane of eukaryote cells, whereas PG exists

only in those of prokaryotes. It is also possible to replace up to 10mol% of DMPC by dimyristoylphosphatidylethanolamine (DMPE) to imitate anionic bacterial membranes. [5, 8, 9]

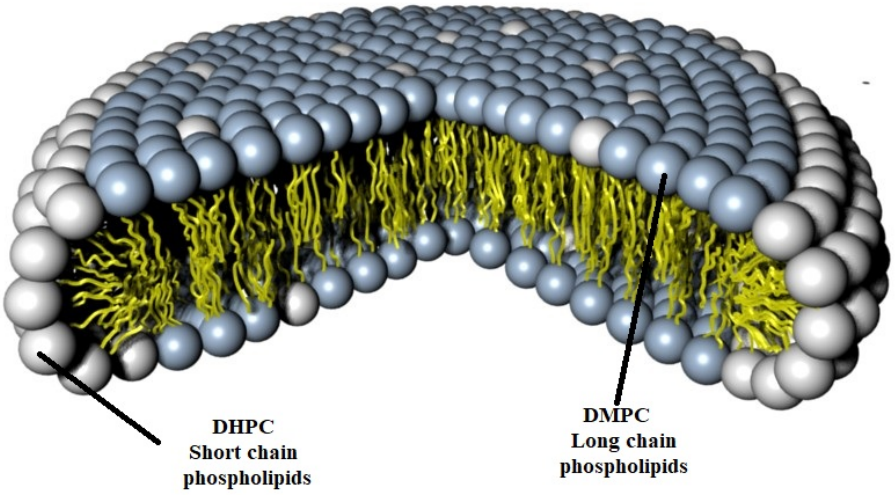

Figure 1.5: 3D structure of the membrane

Chapter 2

NMR Experiments

The NMR experiments are done by using 5mm Probe BBO and 600 MHz Avance NMR spectrometer at NMR Facility at IISER, Mohali. After setting the sample inside the NMR spectrometer, a set of 1-D and 2-D NMR experiments can be done by just changing parameters that are already pre-programmed.

2.1 1D NMR

One dimensional NMR means the spectral data obtained only considering ^1H or ^{13}C or any other single atom. Each 1D experiments divided into two sections- first one is prepared in which spin systems are set to a defined state and the second one is detection which consists of resulting signal. Simple NMR spectra are recorded in solution, and solvent protons must not be allowed to interfere. In NMR, usually Deuterated solvents have been preferred, e.g D_2O. The 1-dimensional NMR plot is between intensity and frequency.

2.2 2D NMR

In 2-dimensional NMR, the intensity is plotted as a function of two frequencies say F_1 and F_2. 2D NMR provides us more information about the compound as compared to 1D NMR and it is very useful in predicting the structure of a compound. The general scheme for 2D NMR is During the first period that is preparation time, the sample is excited by one or more pulses. The resulting magnetization is allowed to evolve for the time t_1 that is evolution time. After that, there is a period of mixing which consists of further more pulses.

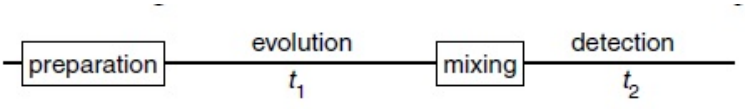

Figure 2.1: General scheme for 2D NMR experiment. Souce: Keeler

The signal is then recorded in the detection time t_2. This sequence of different events is called pulse sequence. [3]

2.2.1 Homonuclear Correlation Experiments

In these type of methods, we observe magnetization transfer between the nuclei of the same type which are connected through bonds.

2.2.1.1 Correlation Spectroscopy (COSY)

It is used to identify spins which are coupled to each other. The spectrum results from COSY experiment show two types of peaks, diagonal peaks, and cross peaks. Diagonal peaks have the same coordinate frequency on each axis and it corresponds to 1D NMR. While cross peaks have different value for each frequency coordinate on each axis. These peaks are symmetrical about the diagonal and it indicates the coupling between the pairs of nuclei which are coupled to each other.

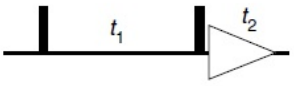

Figure 2.2: Pulse sequence for COSY. Rectangles represent 90^0 angels, Source: Keeler

Consider a weakly coupled two-spin systems. To generate a magnetization along the Y direction (assuming initial magnetization along the Z axis), a 90^0 pulse will be generated along the X-axis.

$$I_{1z} + I_{2z} \xrightarrow{\pi/2\ I_{1x}} \xrightarrow{\pi/2\ I_{2x}} -I_{1y} - I_{2y} \tag{2.1}$$

During time t_1 spin 1 and spin 2 evolve as follows,

$$-I_{1y} \xrightarrow{\Omega_1 t_1 I_{1z}} -cos\Omega_1 t_1 I_{1y} + sin\Omega_1 t_1 I_{1x} \tag{2.2}$$

$$-I_{2y} \xrightarrow{\Omega_2 t_1 I_{2z}} -cos\Omega_2 t_1 I_{2y} + sin\Omega_2 t_1 I_{2x} \tag{2.3}$$

Terms on right then evolve under the coupling as:
For spin 1

$$\begin{aligned} -cos\Omega_1 t_1 I_{1y} + sin\Omega_1 t_1 I_{1x} \xrightarrow{2\pi J_{12} t_1 I_{1z} I_{2z}} (sin\Omega_1 t_1 I_{1x} - cos\Omega_1 t_1 I_{1y}) cos\pi J_{12} t_1 + \\ (sin\Omega_1 t_1 2 I_{1y} I_{2z} + cos\Omega_1 t_1 2 I_{1x} I_{2z}) sin\pi J_{12} t_1 \end{aligned} \tag{2.4}$$

and for spin 2

$$-cos\Omega_2 t_1 I_{2y} + sin\Omega_2 t_1 I_{2x} \xrightarrow{2\pi J_{12} t_1 I_{1z} I_{2z}} (sin\Omega_2 t_1 I_{2x} - cos\Omega_2 t_1 I_{2y}) cos\pi J_{12} t_1 + (sin\Omega_2 t_1 2I_{2y} I_{1z} + cos\Omega_2 t_1 2I_{2x} I_{1z}) sin\pi J_{12} t_1 \quad (2.5)$$

It completes the evolution under t_1. Now following the final 90^0 pulse along X axis and the previous state becomes,

$$(sin\Omega_1 t_1 I_{1x} + sin\Omega_2 t_1 I_{2x}) cos\pi J_{12} t_1 - (2sin\Omega_1 t_1 I_{1y} I_{2z} + sin\Omega_2 t_1 2I_{1z} I_{2y}) sin\pi J_{12} t_1 \quad (2.6)$$

In summary, the 2-dimensional map of COSY is,

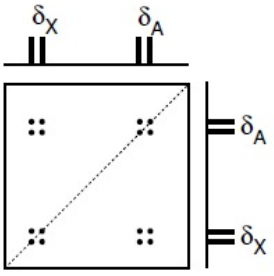

Figure 2.3: COSY map of an AX system. Source: Keeler

Thus cross peaks are dispersed by two different chemical shifts in both dimensions reducing the chance of overlapping of resonances. [3]

2.2.1.2 Total Correlation Spectroscopy (TOSCY)

In this type of spectroscopy, cross peaks are observed not only for nuclei which are directly connected but also between the nuclei which are connected by the chain of couplings. This makes it useful for identifying a larger interconnected network of spin couplings. It is usually used in large molecules with many separated coupling networks such as proteins, peptides, etc. The TOCSY pulse sequence involves a modified spin lock. The spin locking field causes

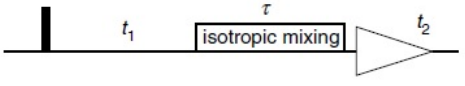

Figure 2.4: Pulse sequence for TOCSY. Source:Keeler

cross-polarization between the two spins which experience identical local RF fields. Thus the spin becomes temporarily equivalent. There are two types of spin-lock sequence, isotropic

mixing and Hartmann-Hahn-mixing (HOHAHA). Isotropic mixing leads to spectra with mixed phase while HOHAHA mixing leads to pure phase spectrum. [3]

2.2.2 Homonuclear through space correlation Experiments

In these type of experiments, coherence transfer occurs through space (dipolar coupling). They exhibit cross peaks for all protons that are close in space.

2.2.2.1 Nuclear Overhauser Effect Spectroscopy (NOESY)

Figure 2.5: Pulse sequence for NOESY. Source:Keeler

NOESY is useful for determining which signals arise from protons that are close to each other in space even if they are not bonded. A NOESY spectrum yields through space correlations via spin-lattice relaxation. NOESY also detects chemical and conformational exchange. [10]

2.2.2.2 Rotating frame Overhauser Effect Spectroscopy (ROESY)

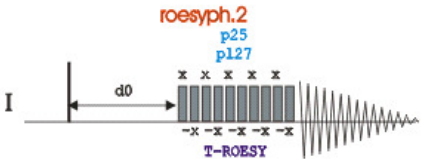

Figure 2.6: Pulse sequence for ROESY. Source: CSIC

ROESY is a type of NOE correlation experiment that is performed in the rotating frame. Its pulse sequence is similar to TOCSY. However, the RF power to achieve spin locking is much lower to TOCSY. In this, intensity increases with correlation time. This is because cross relaxation occurs in the presence of weak field rather than larger static magnetic field. [10]

2.2.3 Heteronuclear through Bond Correlation Experiments

In this type of experiment, we analyze the correlation of two different types of nuclei, (say ^1H and ^{13}C). In the resultant spectra, there will be peaks whose coordinates are given

by chemical shift of one type of nucleus in one dimension(^1H) and chemical shift of another nucleus which is coupled to the first one, in the second dimension(^{13}C).

2.2.3.1 Heteronuclear Single Quantum Correlation (HSQC)

The resulting spectrum in this type of spectroscopy is two-dimensional with one axis for proton (^1H) and the other for a heteronucleus, which is usually ^{13}C or ^{15}N. The spectrum contains a peak for each unique proton attached to the heteronucleus being considered

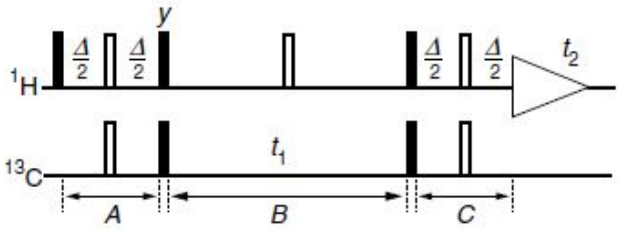

Figure 2.7: Pulse sequence for HSQC. Filled rectangles represent 90 pulses and open rectangles represent 180 pulses. The delay is set to $1/(2J_{12})$; all pulses have phase x unless otherwise indicated. Source: Keeler

The above pulse sequence was to be analyzed by considering each delay and pulse in turn, the resulting calculation would be far too complex to be useful. We start the analysis with spin 1. Assuming the equilibrium magnetization of spin 1 is along z-axis after 90^0 pulse, it becomes -I_{1y}; during period A this then becomes -$2I_{1x}I_{2z}$. Then 90^0(y) pulse to spin 1 turns this to $2I_{1z}I_{2z}$ and 90^0(x) pulse to spin 2 turns it to -$2I_{1z}I_{2y}$. The evolution under period B under offset of spin 2 as follows

$$-2I_{1z}I_{2y} \xrightarrow{\Omega_2 I_{2z} t_1} -cos\Omega_2 t_1 2I_{1z}I_{2y} + sin\Omega_2 t_1 2I_{1z}I_{2x} \tag{2.7}$$

The next two 90 pulses transfer the first term to spin 1;

$$-cos\Omega_2 t_1 2I_{1z}I_{2y} + sin\Omega_2 t_1 2I_{1z}I_{2x} \xrightarrow{\pi/2(I_{1x}+I_{2x})} -cos\Omega_2 t_1 2I_{1y}I_{2z} - sin\Omega_2 t_1 2I_{1y}I_{2x} \tag{2.8}$$

The first term on the right evolves during period C into in-phase magnetization. So the final observable term is cos$\Omega_2 t_1 I_{1x}$. [3]

2.2.3.2 Heteronuclear Multiple Bond Correlation

In this type of spectroscopy we study the correlation between proton and other nucleus only for those which are connected by two or three bonds. It can show correlations between amide hydrogen to α proton.

Chapter 3

Conformational Studies of AMP's

3.1 Mechanism of Action of AMP's

Antimicrobial peptides (AMP's) firstly discovered in 1950. It is one of the greatest discovery of the 20^{th} century and have been used with great success to treat microbial infections. In today's world there are more than 8000 sequences of peptides and every peptide shows different variations in sequence, length and structure but the 3-dimensional structures can only been characterized of 13% of AMP's which were determined by solution state NMR spectroscopy. The antimicrobial peptides are of different types like helical, β-strand and mixed. According to CAMP (Collection of antimicrobial peptides) database, till now 757 high resolution AMP structures have been determined. The majority of these AMP's are helical. The diversity of AMP's structures suggests that the mechanism of action of these peptides on the target cells can be complex and beyond the pore mechanism based on helical structures which have been widely adopted in the design and development of AMP exhibiting antimicrobial activities. [11]

Structure activity relationship studies of AMP shows that there are many factors like charge, secondary structure, hydrophobicity, hydrophobic moment and amphipathicity that affects the specificity and biological activity of these peptides. These all factors are so interdependent on each other that if we alter one property, it will result in significant change to one or more of the other factors. Analysis of membrane structure changes during AMP binding from initial interaction of AMP's with their target membrane. Conformation changes upon interaction, accumulation of critical concentration and self-association and direct mechanism of action from pore formation to general disruption of the cell membrane to downstream effects that lead to the death of the cell. [12]

Mechanism of Action of AMP's was studied on various membrane models with fewer studies focusing on action of AMP's on whole microbial cells. These studies show the primary interaction of these peptides with the cell membrane. In our case, we use bicelle which acts as a mimic to the cell and these interactions can be classified in two different categories: membrane disruptive and non-membrane disruptive. The proposed models for mechanism of action extends from pore formation to general membrane disruption to the structure rearrangements such as molecular shape. AMP initially are in unstructured state in solution. The initial interaction is brought via electrostatic interactions between cationic residues and negatively

charged lipids in the bacterial membrane target. [13, 14, 15]

3.2 Structure determination by NMR

NMR spectroscopy enables the determination of peptide or protein structure in solution state. In single crystal diffraction we need the protein to be crystallized but in this case, we don't need of it. Also, spin physics changes with increasing molecular weight, due to which the analysis of protein having molecular weight greater than 50KDa presents as a major challenger in the field. Structure determination using NMR depends on the so-called nuclear overhauser effect. The magnitude of NOE depends not only on the distance separation of the interacting spins but also on its motional properties.

$$NOE \approx r^{-6}.f(\tau_c) \tag{3.1}$$

τ_c stands for correlation time, the time molecule needs to rotate by 360^0 about an arbitrary axis. NOESY spectrum consists of all the information about the spatial proximities of protons and therefore encoded the three-dimensional arrangement of atoms and the structure.

3.2.1 Steps to determine structure by NMR

- Production of the peptide.
- Establishment of suitable conditions for recording NMR spectra of peptide or protein (like stable over time at chosen pH and temperature).
- Measurement of different different 2-dimensional and 3-dimensional NMR spectra.
- Sequential specific assignment of all non-labile proton frequencies.
- Assignment of all the cross-peaks in TOCSY and NOESY spectra.
- Collecting all constraints like dihedral angles, inter-nuclei distance, amide-proton exchange rate, chemical shifts index.
- Structure calculation using distance geometry.
- Validation of structure in the protein database.

3.3 Measurement of Spectra

In order to assign the NOE (known as NUclear Overhauser Effect) to specific resonances, all non-labile protons must be assigned to their sequence-specific position in the sequential resonance assignment. As there are a large number of protons per residue (3-13) and

the resulting resonance overlap, peptides cannot be assigned from 1D spectra even smaller peptides. To assign them we require two or three-dimensional correlation spectra of the peptides. The following figure indicates the positions of the protons in the 1D spectrum:

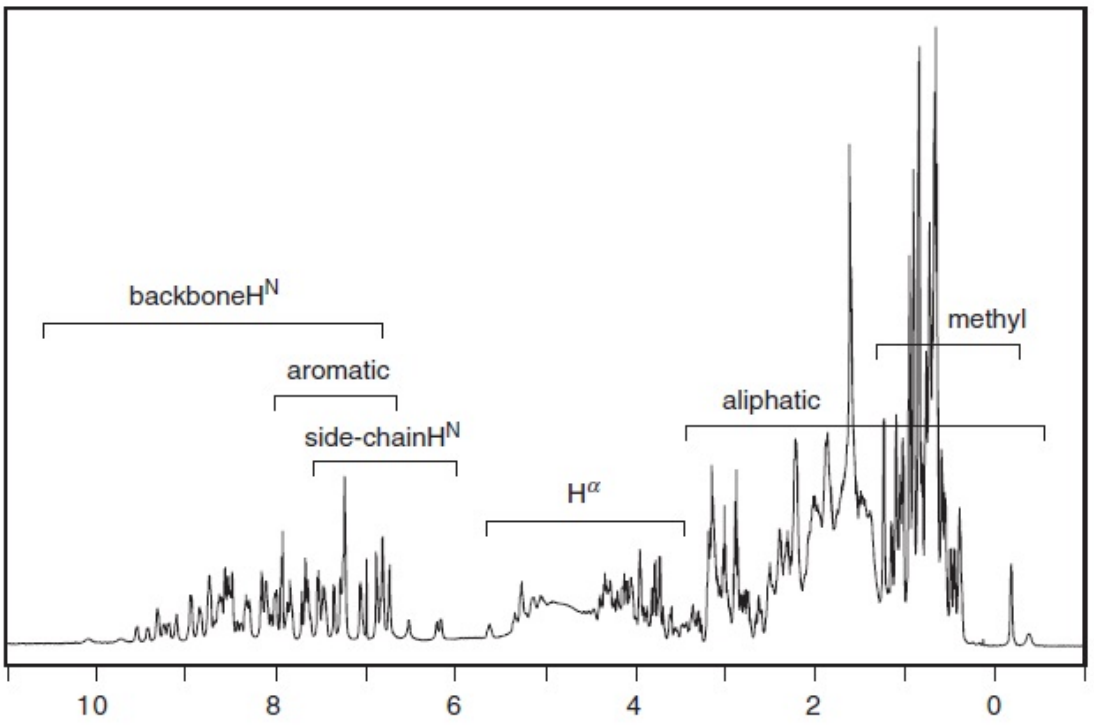

Figure 3.1: Chemical shift positions of chemical groups. Source: Cavanagh- Protein NMR Spectroscopy

For resonance assignment of small non-labeled peptides, generally set of three different spectra is recorded name as COSY, TOCSY, NOESY. The spectra's usually recorded in 90% D_2O + 10% H_2O. The very strong water signal must be experimentally suppressed and the residual water usually appears in the middle of the spectrum. In 2D spectra, the residual water signal is manifested as a band of noise in the center of the spectrum. It may obscure peaks close to the water resonance (such as the Hα protons). [16, 17]

3.3.1 Rules to classify cross peaks in spectra

Actually, there are some rules to classify the positions of cross peaks in 2-dimensional spectra.

3.3.1.1 Correlation Spectroscopy (COSY)

See Figure 3.2 for the positions:

a. all non-labile, non-aromatic sidechain protons except those from βH-γCH_3 of Thr, δH-δH of Pro and βH-βH of Ser.

b. αH-βCH_3 of Ala and βH-γCH_3 of Thr.

c. αH-βH of Val, Ile, Leu, Glu, Gln, Met, Pro, Arg, and Lys.

d. αH-βH of Cys, Asp, Asn, Phe, Tyr, His and Trp.

e. αH-αH of Gly, αH-βH of Thr, δH-δH of Pro, αH-βH and βH-βH of Ser.

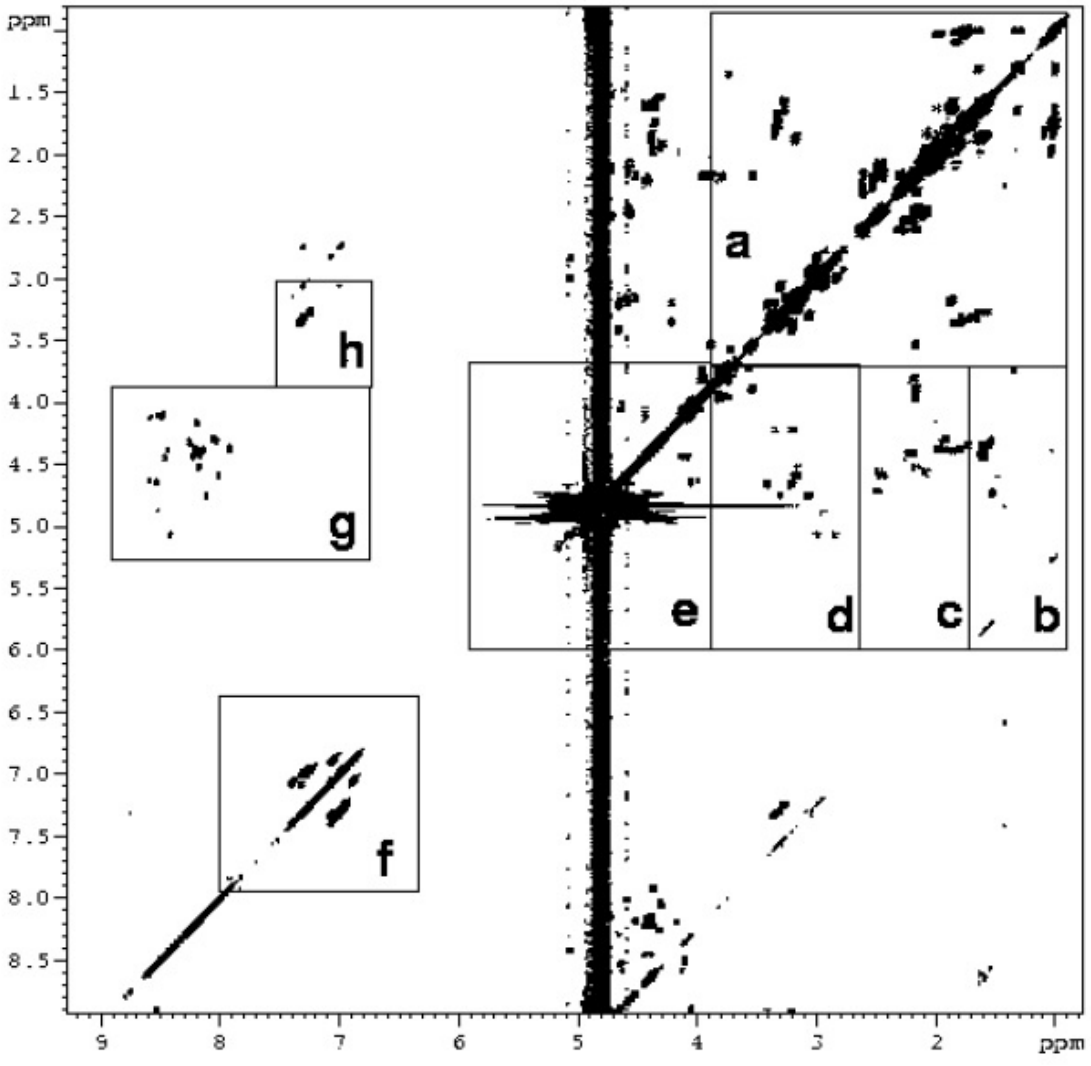

Figure 3.2: [^1H-^1H]-COSY Spectra, Source: Cavanagh- Protein NMR Spectroscopy

f. aromatic ring protons, including 2H-4H of His, as well as sidechain protons from Asn and Gln.

g. backbone NH-αH, this region is also called fingerprint region.

h. δCH_2-ϵNH of Arg.

Scalar couplings can only be observed between protons that are separated by not more than three bonds. Moreover, the protons need to have a different resonance frequency. [16, 18]

3.3.1.2 Total Correlation Spectroscopy (TOCSY)

For this type of spectroscopy, we follow Figure:3.3 basically called as TOCSY fingerprint. In this, all amino acids have different patterns in amino acid residues, because there is no scalar coupling across the amide bond.

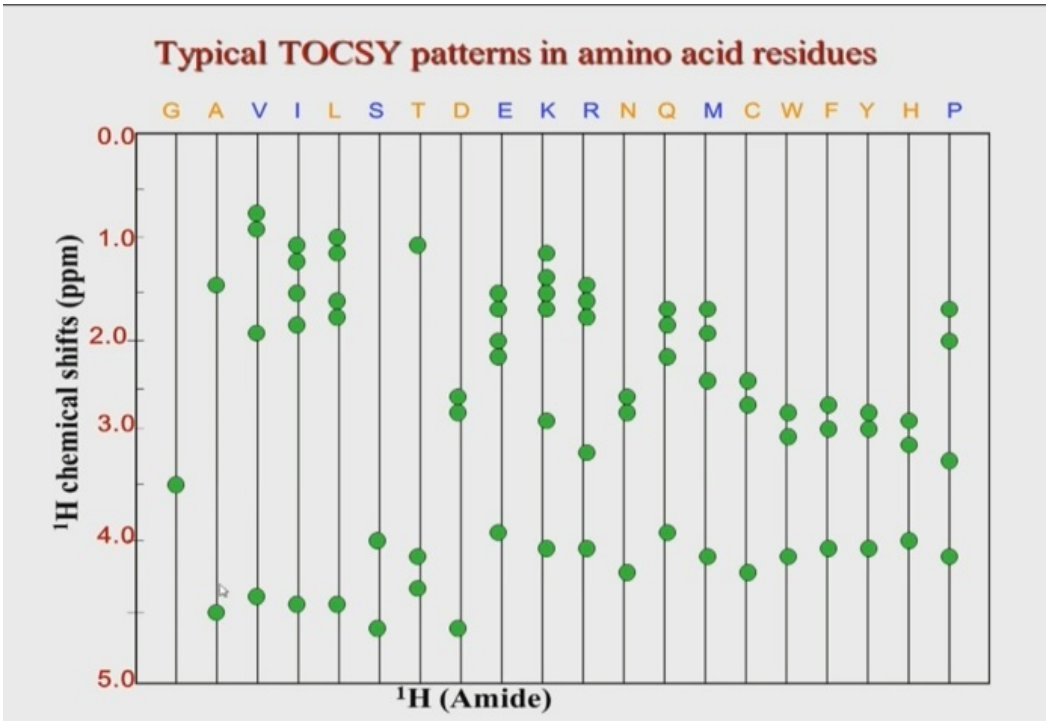

Figure 3.3: TOCSY Fingerprint. Source: Youtube-Principles and Applications of NMR Spectroscopy

Analysis of all the spin systems allows us to decide which amino acids belong to which spin system. Possible criteria are, Occurrence or absence of methyl groups, length of the spin system, positions of chemical shifts in the spin system and mixing time (this parameter determines whether it is neighboring correlations or long-distance correlations. This parameter is generally used to determine in the region where there is smaller overlap. [20, 21]

3.4 Resonance assignment of non-labeled peptides

3.4.1 4.1 Optimizing spectral quality

The spectral quality of the peptide can be calculated by the inspection of the fingerprint region in which we will analyze a number of peaks that roughly match the number of non-proline residues, if there are more than 10% of peaks are missing, in that case, the conditions should be varied like temperature, pH, salt, etc. in order to remove peak overlap or aggregation Sometimes it is advisable to record the second set of spectra at a slightly different temperature to remove peak overlap. [16, 18, 21]

3.4.2 Spin system Identification

The spin systems are classified according to the first step. The table below contains the random coil chemical shifts of all amino acids calculated from the structured proteins, peptides present in the database of BMRB.

Table 3.1: 1H NMR Random coil chemical shifts of amino acids (Source: BMRB) (Relative to DSS, ppm)

Residue	α**H**	β**H**	**Others**
Ala	4.25	1.35	-
Arg	4.29	1.79, 1.76	γCH_2 1.56, 1.54; δCH_2 3.11, 3.09; εNH 7.45
Asn	4.66	2.80, 2.74	δNH_2 7.34, 7.14
Asp	4.59	2.72, 2.67	-
Cys	4.68	3.15, 3.07	γCH_2 1.99
Gln	4.27	2.04, 2.01	γCH_2 2.31, 2.29; δNH_2 7.21, 7.04
Glu	4.24	2.02, 1.99	γCH_2 2.26, 2.24
Gly	3.96	-	-
His	4.62	3.16, 3.10	2H 7.82; 4H 7.17
Ile	4.17	1.78	γCH_2 1.26, 1.19; γCH_3 0.77; δCH_3 0.67
Leu	4.31	1.61, 1.52	γCH 1.50; δCH_3 0.75, 0.72
Lys	4.26	1.77, 1.74	γCH_2 1.36, 1.35; δC$H_2$1.61, 1.59; εCH_2- 2.91,2.90; εNH 7.32
Met	4.41	2.02, 1.99	γCH_2 2.36, 2.33; εCH_3 1.74
Phe	4.62	2.99, 2.93	2,6H 7.04; 3,5H 7.06; 4H 6.99
Pro	4.39	2.07, 1.99	γCH_2 1.92,1.89; δCH_2 3.63, 3.60
Ser	4.48	3.87, 3.84	-
Thr	4.45	4.16	γCH_3 1.14
Trp	4.68	3.18, 3.12	2H 7.27; 4H 7.65; 5H 7.18; 6H 7.25; 7H 7.50
Tyr	4.61	3.03, 2.95	2,6H 6.92,6.91; 3,5H 6.69
Val	4.17	1.98	γCH_3 0.82, 0.80

The spin systems which are long enough like Lys, Arg, Met, Gln, Glu and Pro contains two γ protons, which are coupled to β protons. Usually, the β protons are observed at frequencies higher than 2.2 ppm and were therefore called as U (upfield) spin systems. γH

frequencies of Met, Glu, Gln are lower than those of β protons whereas for Arg, Lys, Pro, Leu are higher.

3.4.3 Extraction of structural information

The structural information can be collected by measuring different constrains using

- Interproton distances (NOE $\propto R^{-6}$)
- Dihedral angles (J-coupling and Karplus equations)
- Chemical Shift Index
- Hydrogen Bonding (Amide proton exchange rates)

The most important as a part of structure determination is Karplus relations, it describes the correlation between J-coupling constants and dihedral torsion angles, following are the Karplus equation:

$$^3J_{NH\alpha} = 6.4cos^2\theta - 1.4cos\theta + 1.9 \tag{3.2}$$

$$^3J_{\alpha\beta} = 9.5cos^2\theta - 1.6cos\theta + 1.8 \tag{3.3}$$

$$^3J_{N\beta} = -4.4cos^2\theta + 1.2cos\theta + 0.1 \tag{3.4}$$

$$^3J_{C'\beta} = 8.0cos^2\theta - 2.0cos\theta \tag{3.5}$$

where as ^{3}J is the coupling constant and θ is the dihedral angle. [28, 29, 30]

Chapter 4

Spectral Analysis and Results

4.1 Preliminary analyzed chemical shifts

The following table summarized the preliminary analyzed chemical shifts of amino acids present in diptericin at 298K.

Table 4.1: 1H NMR Chemical Shifts of amino acids present in diptericin. (Relative to DSS, ppm)

Residue	**αH**	**βH**	**Others**
Ala	4.25	1.375	-
Arg	4.29	1.79, 1.76	γCH_2 1.56, 1.54; δCH_2 3.11, 3.09; εNH 7.45
Asn	4.66	2.88, 2.73	δNH_2 6.94
Asp	4.59	2.65, 2.49	-
Gln	4.27	2.18, 2.19	γCH_2 2.31, 2.29; δNH_2 7.21, 7.04
Glu	4.24	2.02, 1.99	γCH_2 2.26, 2.24
Gly	3.85	-	-
His	4.62	3.16, 3.10	2H 7.83; 4H 7.29
Ile	4.17	1.78	γCH_2 1.26, 1.19; γCH_3 0.77; δCH_3 0.67
Leu	4.31	1.61, 1.52	γCH 1.50; δCH_3 0.75, 0.72
Lys	4.26	1.77, 1.74	γCH_2 1.49, 1.51; δCH_2 1.60, 1.58; εCH_2- 2.92,2.91; εNH 7.32
Phe	4.62		3,5H 7.36; 4H 7.30
Pro	4.39	2.07, 1.99	γCH_2 1.92,1.89; δCH_2 3.65, 3.64
Ser	4.47	3.92, 3.90	-
Thr	4.42	4.22	γCH_3 1.27
Trp	4.67		2H 7.24; 4H 7.64; 5H 7.14; 6H 7.22; 7H 7.49
Tyr	4.58	2.89, 3.04	2,6H 7.03; 3,5H 6.72
Val	4.22	1.96	γCH_3 0.84, 0.82

Chemical shifts of αH protons of diptericin when compared to chemical shifts from random coil values shows a difference between them. This provides a first indication of the presence of its secondary structure. [26, 27]

4.2 Spectral Assignment

To determine the mechanism of action and structure of diptericin, we did spectral analysis of three different samples we had prepared namely,

1. Diptericin in 90% H_2O + 10% D_2O
2. Negative bicelle
3. Diptericin in negative bicelle

Following are the spectral analysis of both 1D and 2D experiments of the above samples:

4.2.1 Diptericin in 90% H_2O + 10% D_2O

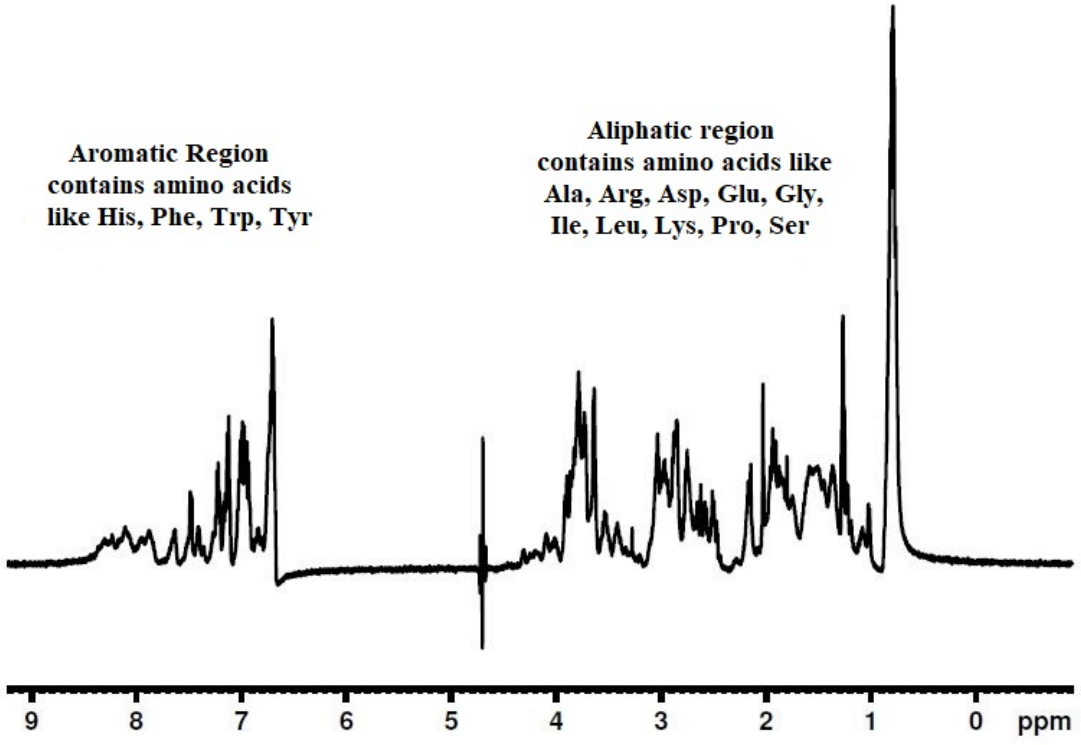

Figure 4.1: 1D ^1H spectra of diptericin in 90%H_2O + 10%D_2O

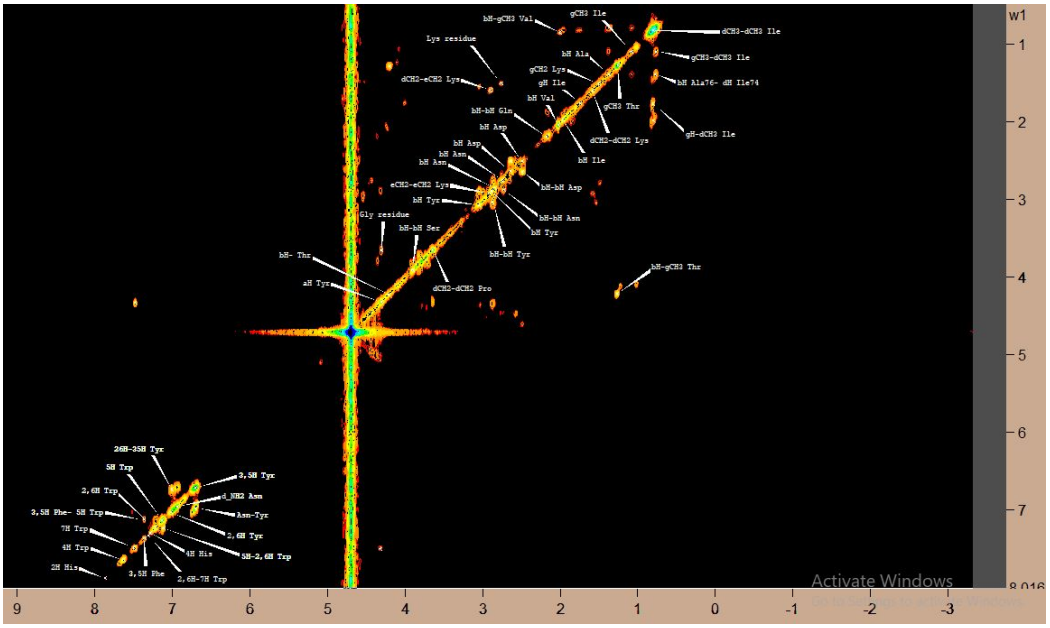

Figure 4.2: 2D ^{1}H-^{1}H COSY spectra of diptericin in $90\%H_2O + 10\%D_2O$

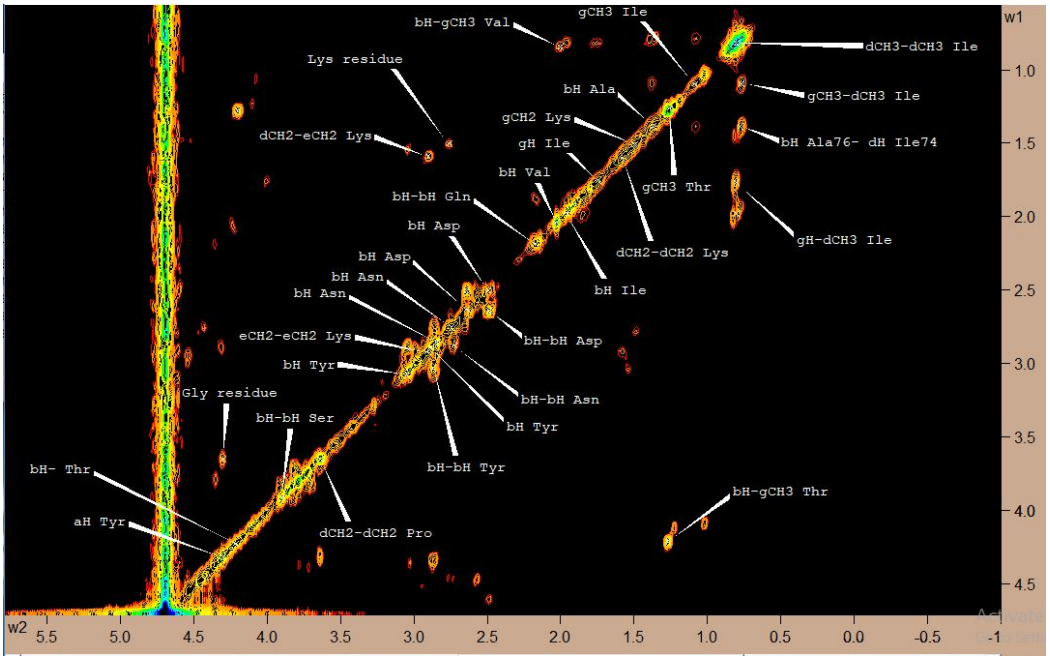

Figure 4.3: 2D ^{1}H-^{1}H COSY spectra of aliphatic region of diptericin in $90\%H_2O$+$10\%D_2O$

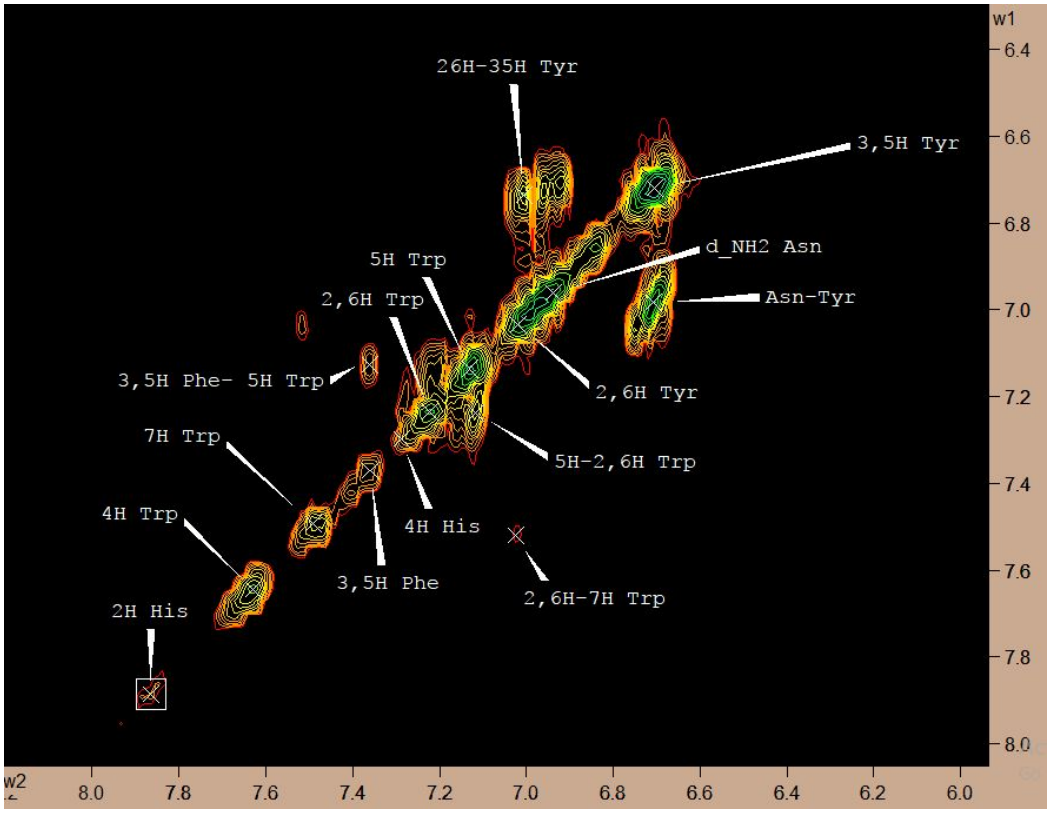

Figure 4.4: 2D ^1H-^1H COSY spectra of aromatic region of diptericin in $90\%H_2O$+$10\%D_2O$

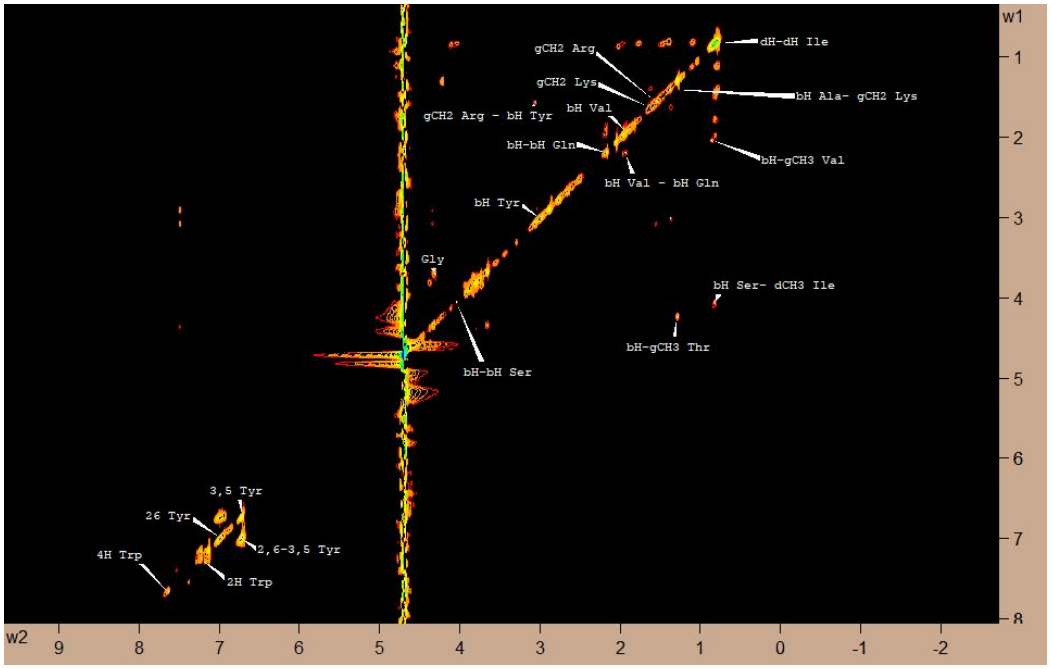

Figure 4.5: 2D ^1H-^1H TOCSY spectra of diptericin in $90\%H_2O + 10\%D_2O$

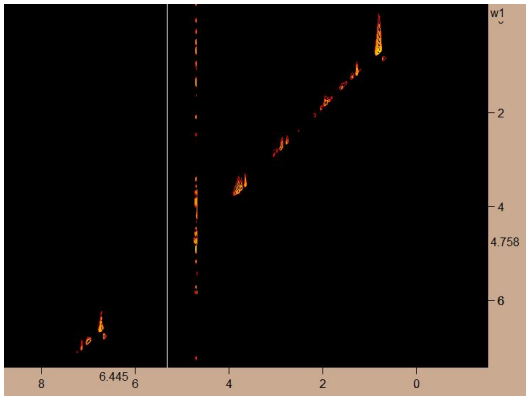

Figure 4.6: 2D ^{1}H-^{1}H NOESY spectra of diptericin in $90\%H_2O + 10\%D_2O$

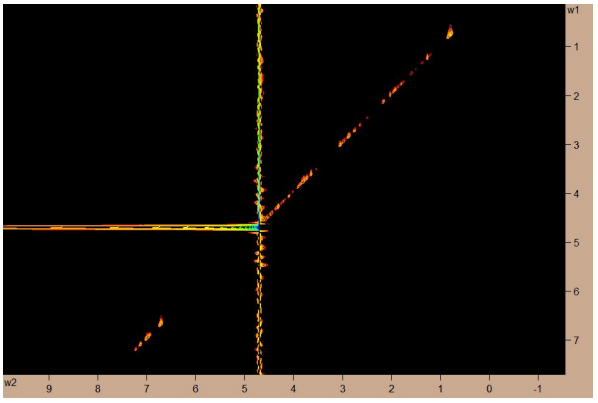

Figure 4.7: 2D ^{1}H-^{1}H ROESY spectra of diptericin in $90\%H_2O + 10\%D_2O$

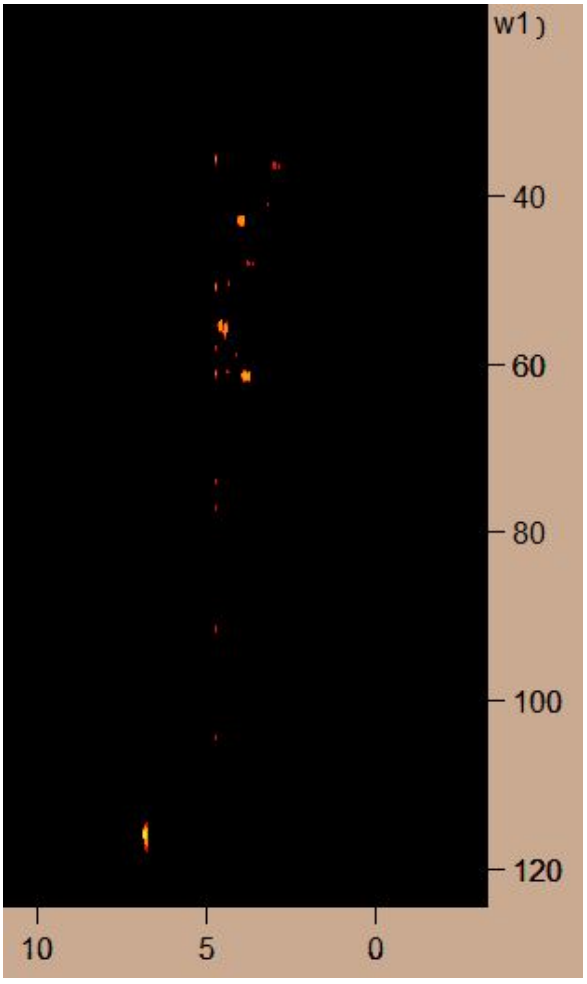

Figure 4.8: 2D ^{1}H-^{13}C HSQC spectra of diptericin in $90\%H_2O + 10\%D_2O$

4.2.2 Negative Bicelle

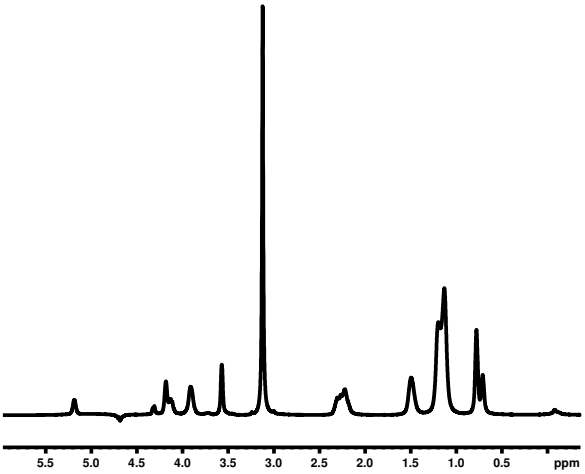

Figure 4.9: 1D ^{1}H spectra of [DMPC][DMPG][DMPE]/[DHPC] Negative Bicelle in phosphate buffer of pH 6.6

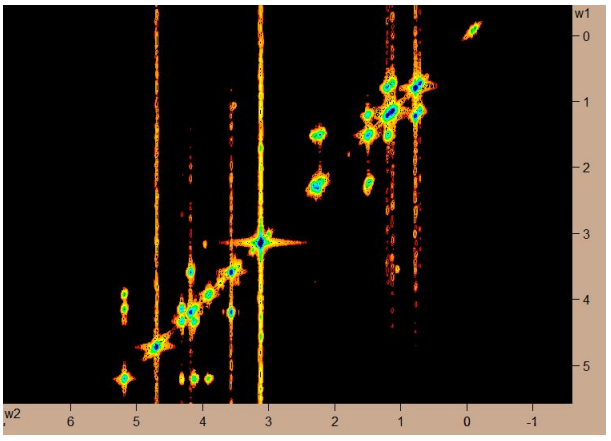

Figure 4.10: 2D ^{1}H-^{1}H COSY spectra of [DMPC][DMPG][DMPE] / [DHPC] Negative Bicelle in phosphate buffer of pH 6.6

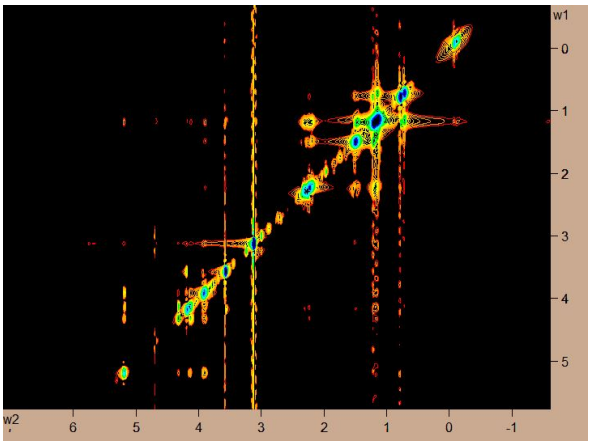

Figure 4.11: 2D ^{1}H-^{1}H TOCSY spectra of [DMPC][DMPG][DMPE] / [DHPC] Negative Bicelle in phosphate buffer of pH 6.6

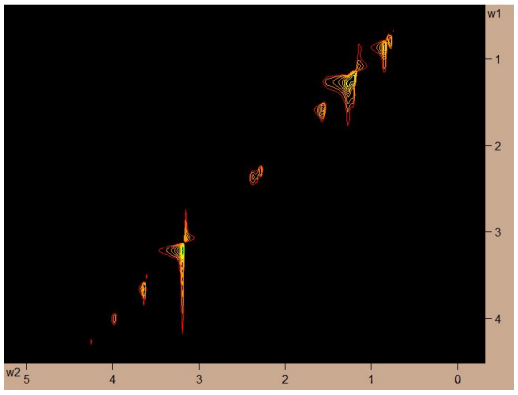

Figure 4.12: 2D ^{1}H-^{1}H NOESY spectra of [DMPC][DMPG][DMPE] / [DHPC] Negative Bicelle in phosphate buffer of pH 6.6

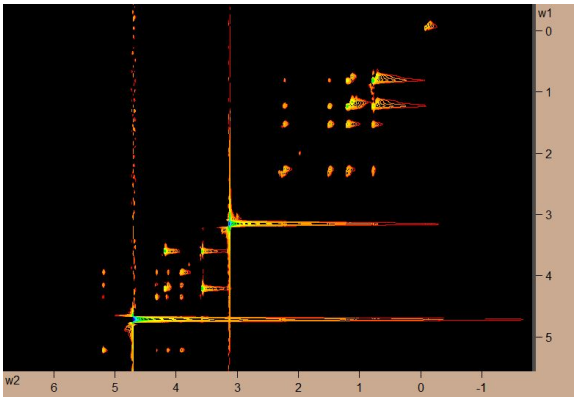

Figure 4.13: 2D ^{1}H-^{1}H ROESY spectra of [DMPC][DMPG][DMPE] / [DHPC] Negative Bicelle in phosphate buffer of pH 6.6

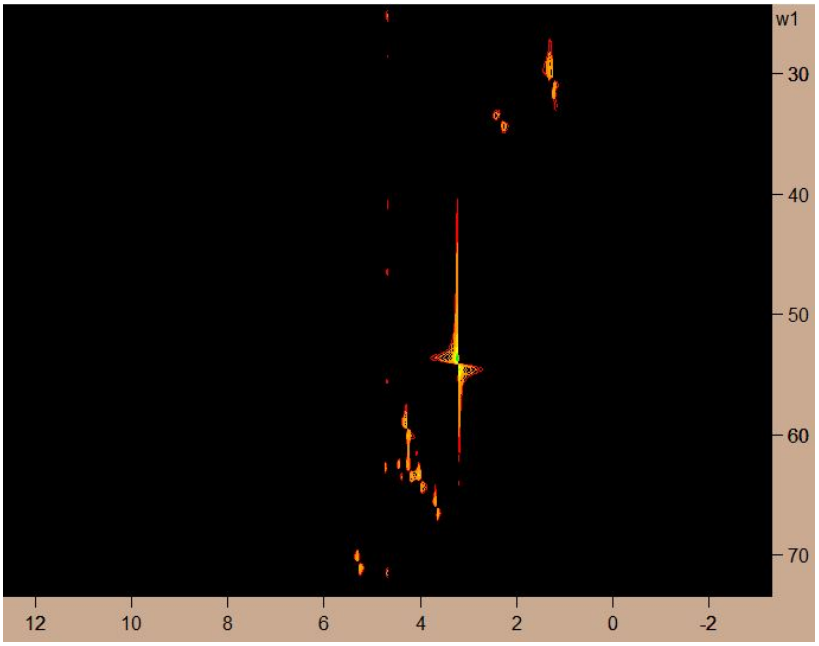

Figure 4.14: 2D ^{1}H-^{13}C HSQC spectra of [DMPC][DMPG][DMPE]/[DHPC] Negative Bicelle in phosphate buffer of pH 6.6

4.2.3 Diptericin in negative bicelle

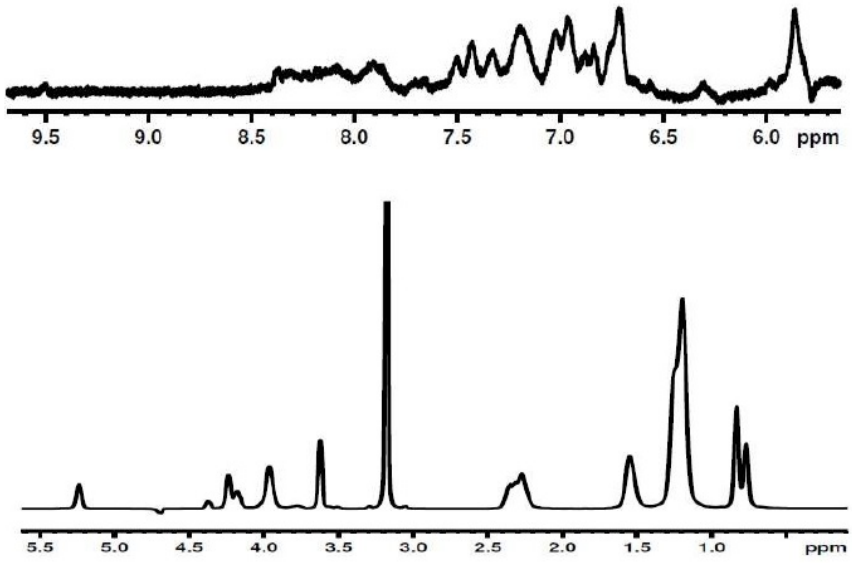

Figure 4.15: 1D ^{1}H spectra of diptericin in negative bicelle (From 0 to 5.5ppm its aliphatic region and from 5.5 to 9.5 its aromatic region)

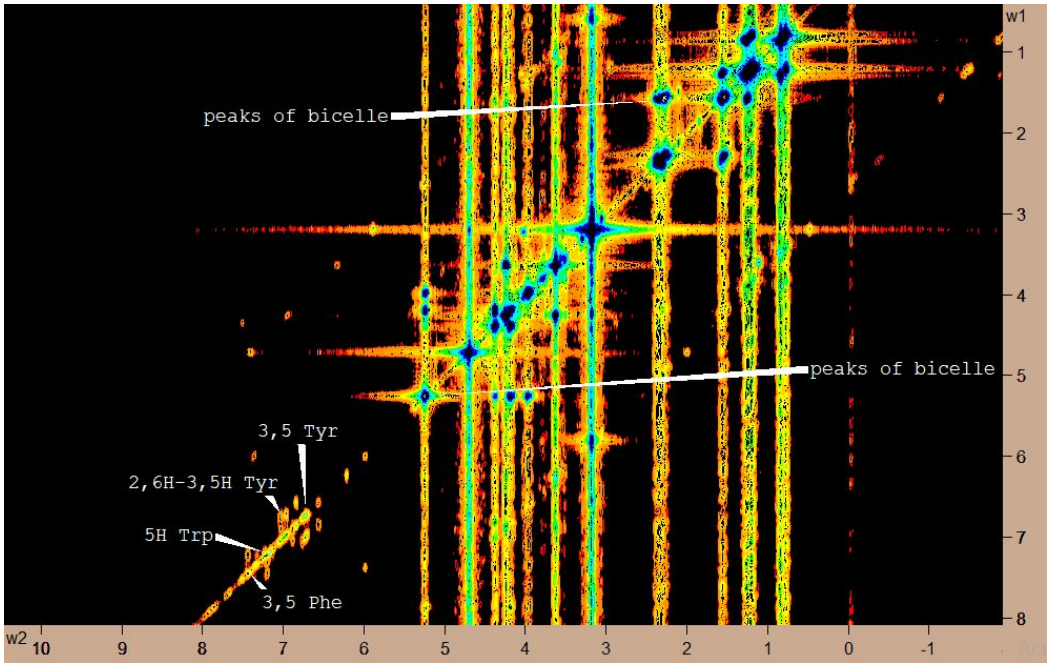

Figure 4.16: 2D ^{1}H-^{1}H COSY spectra of diptericin in negative bicelle (Dark blue peak in an aliphatic region are of negative bicelle)

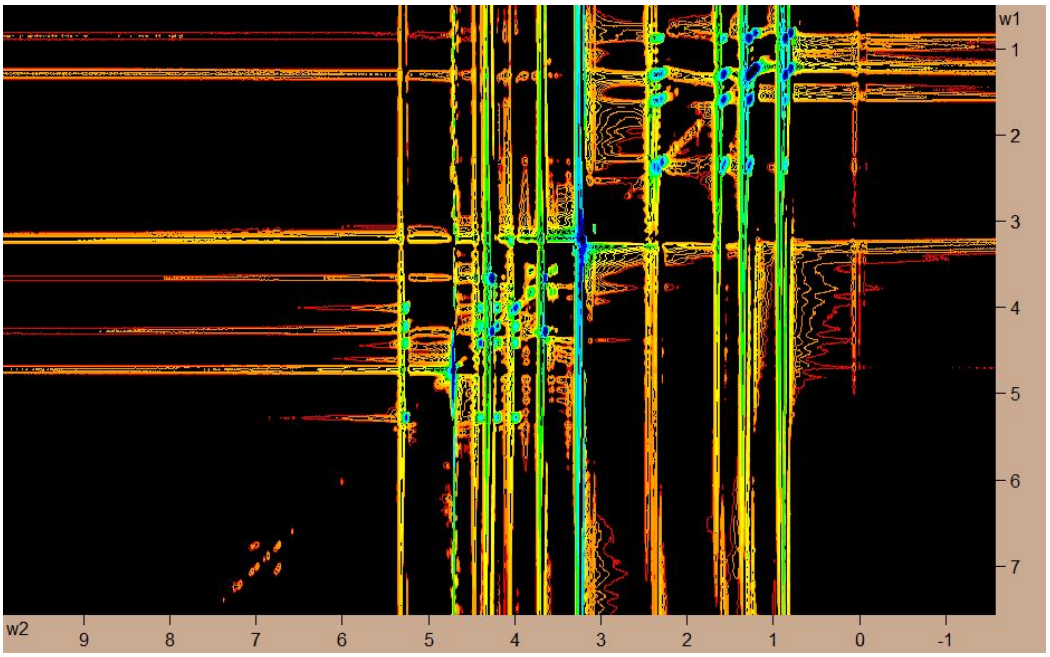

Figure 4.17: 2D ^{1}H-^{1}H TOCSY spectra of diptericin in negative bicelle (Dark blue peak in an aliphatic region are of negative bicelle)

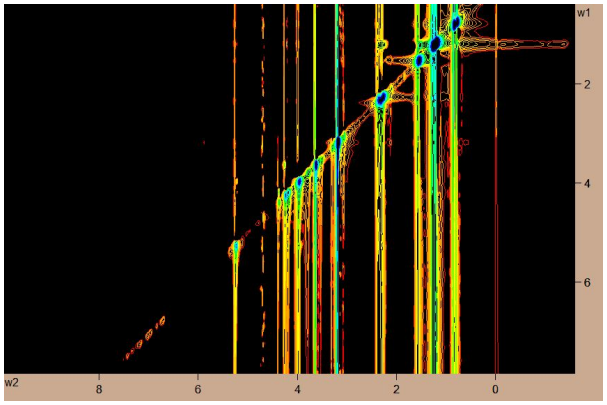

Figure 4.18: 2D ^{1}H-^{1}H NOESY spectra of diptericin in negative bicelle (Dark blue peak in an aliphatic region are of negative bicelle)

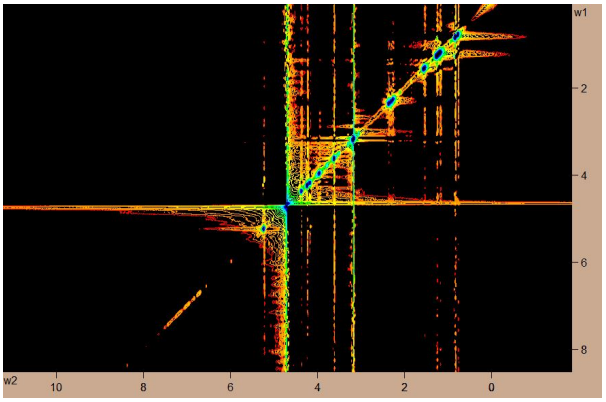

Figure 4.19: 2D ^{1}H-^{1}H ROESY spectra of diptericin in negative bicelle (Dark blue peak in an aliphatic region are of negative bicelle)

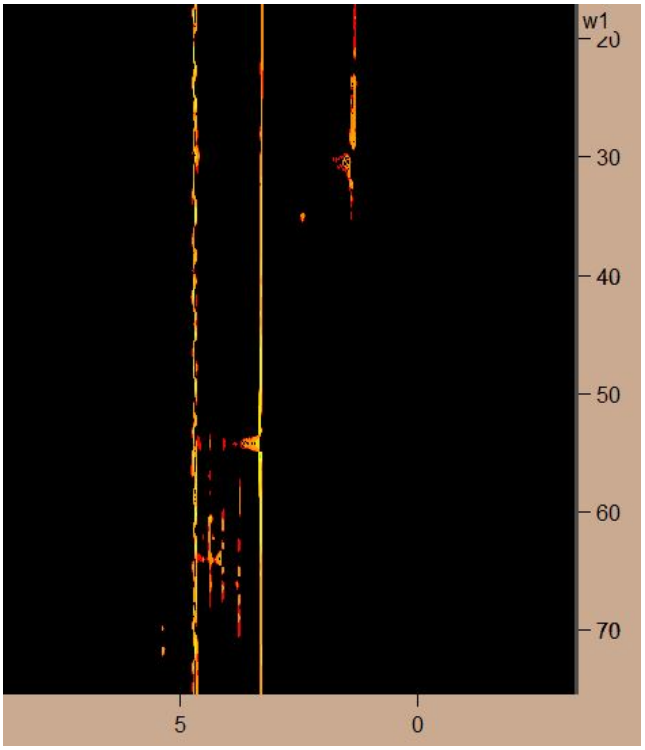

Figure 4.20: 2D ^{1}H-^{13}C HSQC spectra of diptericin in negative bicelle

4.2.4 Comparison of Spectra

Following are the comparisons of 1D spectra of samples, diptericin in 90% H_2O + 10% D_2O and diptericin in negative bicelle,

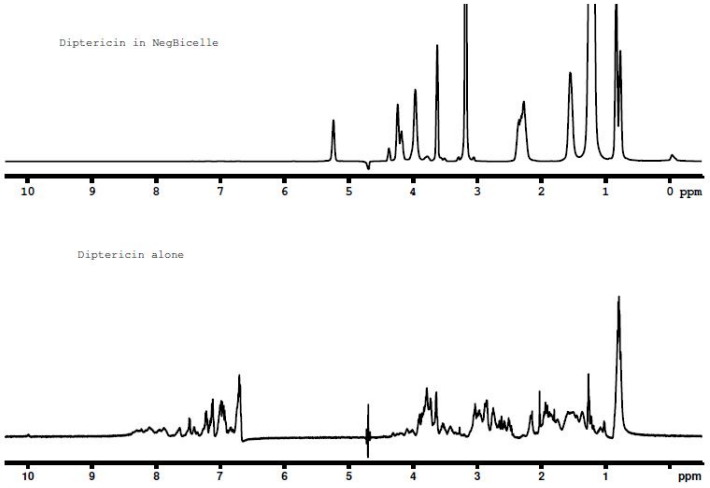

Figure 4.21: Comparison of Full 1D Spectra of diptericin in two different environments

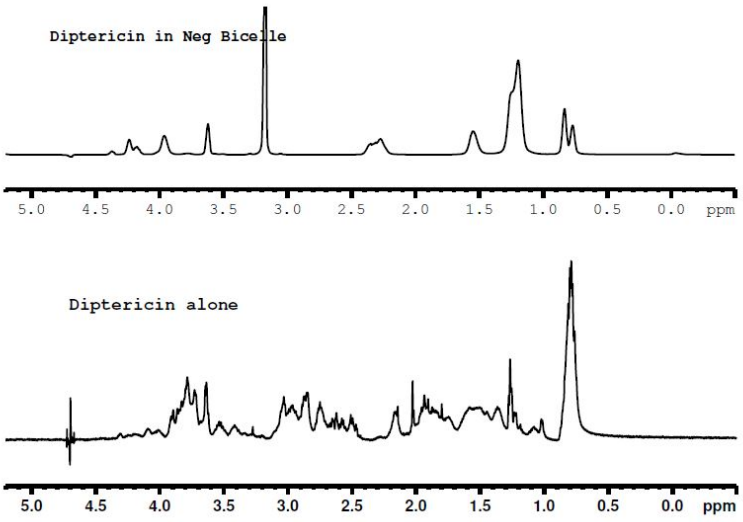

Figure 4.22: Comparison of 1D Spectra of diptericin in two different environments part 1 from δ-(0.0-5.0ppm)

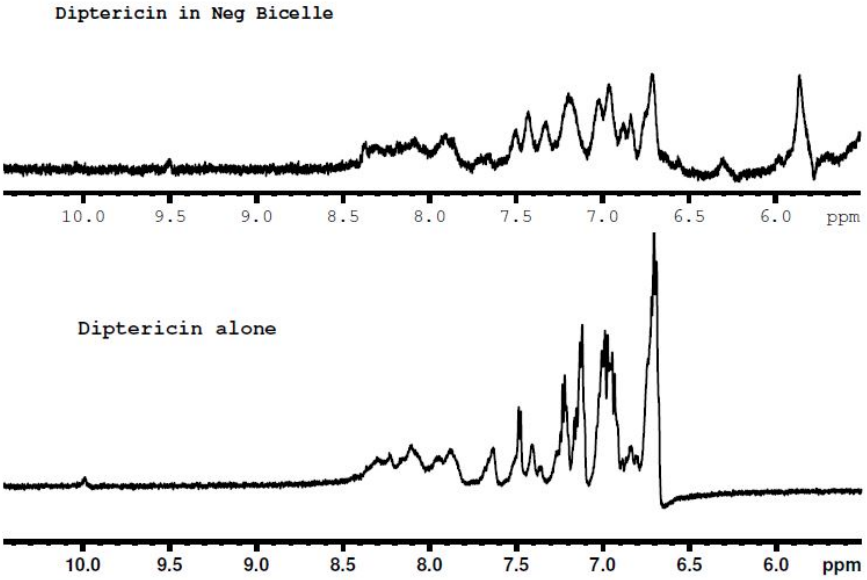

Figure 4.23: Comparison of 1D Spectra of diptericin in two different environments part 2 from δ-(5.5-10.0ppm)

4.3 Conclusion

In the above section 4.2.4, we compared the spectra of diptericin in 90% H_2O + 10% D_2O and diptericin of negative bicelle. In Figure 4.21, we can see that kind of peaks we are observing in the 1D spectra of diptericin alone are different from the peaks in 1D spectra of diptericin in negative bicelle which indicates the interaction of peptide with bicelle membrane. After enlarging the aliphatic region i.e. from δ (0-5.5 ppm) in both the samples (refer to Figure 4.22), we observe that the peaks in sample of diptericin in negative bicelle contain the peaks of bicelle only (refer to Figure 4.9), and amino acid peaks are missing which shows that diptericin did not enter the bicelle membrane in this region. But in case of the aromatic region i.e. from δ (5.5-9 ppm) (refer to Figure 4.23) we observed the similar kind of peaks in both the samples, which indicates that it might be partially entering or pores the cell membrane. We also observed COSY, TOCSY, NOESY etc. spectra (refer to Figure 4.16, 4.17, 4.18) which confirms our results that diptericin partially enters the bicelle membrane. Most of the protons of amino acids had been labeled using the NMR spectral assignment techniques (refer to Figure 4.2, 4.3, 4.4, 4.5 and 4.16).

Chapter 5

Summary and Future directions

Our aim was to study the conformational studies of 82-amino acids long antimicrobial peptide diptericin inside a bicelle and to determine its secondary structure. Firstly, it is difficult to study with unlabeled and 82 residues long peptide. So for that, it should important for someone to study about smaller known peptide first. In this particular case, we studied drosocin (19-amino acids peptide). Generally, The mechanism of action of any peptide in bicelle can be examined by comparing the spectra of peptide alone in 90% H_2O + 10% D_2O and peptide in different bicelle environment. For this study, we prepared negative bicelle containing longer acyl chain lipids DMPC, DMPE, DMPG and short acyl chain lipid DHCP with a q value of 0.5 for drosocin and 0.769 for diptericin (as mentioned in chapter 1.6). Here q defines the molar ratio of long and short chain lipids. After this, we performed 1D and 2D spectra of three different samples, negative bicelle alone, diptericin alone and diptericin in negative bicelle at 298K. We used the peptide drosocin for the reference and perform all the experiments with drosocin to get familiar with a NMR spectrometer and structure analysis software.

NMR experiments with diptericin in negative bicelle show that there are no peaks of amino acids in the aliphatic region of the sample but in case of the aromatic region, we are getting similar kind of peaks of amino acids as we got in the diptericin alone sample. This result gives us very important information about the interaction between bicelle and protein from which we can conclude that diptericin might be partially entering the cell membrane.

We did the spectral analysis of diptericin as shown in the chapter 4, and from COSY and TOCSY spectral assignment we saw the interaction between Ala-Ile, Ser-Ile, Ala-Lys, Arg-Tyr and many more amino acids and from that we got a preliminary analyzed chemical shift table 4.1 which we will use in the structure prediction software to determine its secondary structure.

In future, as a part of structure determination we also need complete backbone assignment which contains NH-αH protons as shown in region "g" of Fig. 3.2. These can be obtained from the analysis of four types of triple resonance experiments HNCO, HNCA, HN(CO)CA and HN(CA)CO.
In addition, we want to study the folding mechanism and structure formation of diptericin, this can be done after collecting all constraints like inter-nuclei distances using NOE effect, dihedral angles, amide proton exchange rate, and the final chemical shift index as given in Table 4.1 using MARDIGAS and then will put all these things in computer-based software like CYANA to get its final structure.

Appendix A

Three letter codes for amino acids

Amino Acids	Symbol	Three letter code
Alanine	A	Ala
Arginine	R	Arg
Asparagine	N	Asn
Aspartic acid	D	Asp
Cysteine	C	Cys
Glutamine	Q	Gln
Glutamic acid	E	Glu
Glycine	G	Gly
Histidine	H	His
Isoleucine	I	Ile
Leucine	L	Leu
Lysine	K	Lys
Methionine	M	Met
Phenylalanine	F	Phe
Proline	P	Pro
Serine	S	Ser
Threonine	T	Thr
Tryptophan	W	Trp
Tyrosine	Y	Tyr
Valine	V	Val

Appendix B

Processing commands used in Sparky

Sparky helps us to assign and integrate peaks in NMR spectra. The output is the list of the assigned peaks, chemical shifts, etc.

- ct - countour levels
- F8 - add peaks from the spectra
- F10 - integrate the peaks
- pc - peak center
- at - assignment dialog box
- lt - peak list
- rl -resonance list
- aD - delete assignment
- rr - rename group or atoms
- oc - ornament copy
- op - ornament paste
- ot - ornament properties box
- pg - set of selected peaks into one group called peak group

Bibliography

[1] H. Friebolin, Basic one- and two-dimensional NMR spectroscopy, Wiley-VCH Verlag GmbH and Co. KGaA, 2011

[2] Banwell and McCash, Fundamentals of Molecular Spectroscopy, Tata McGraw Hill, 1994.

[3] James Keeler, Understanding NMR Spectroscopy, Wiley, 2014, Second edition

[4] Guangshun Wang, Structural Biology of Antimicrobial Peptides by NMR Spectroscopy, Current Organic Chemistry, Volume 10 , Issue 5 , 2006

[5] Scott WR, Baek SB, Jung D, Hancock RE, Straus SK., NMR structural studies of the antibiotic lipopeptide daptomycin in DHPC micelles., Biochim Biophys Acta. 2007 Dec;1768(12):3116-26. Epub 2007 Sep 15.

[6] M. Cudic, P. Bulet, R. Hoffmann, D. J. Craik and L. Otvos Jr, Chemical synthesis, antibacterial activity and conformation of diptericin, an 82-mer peptide originally isolated from insects, Eur. J. Biochem, 266, 549-558(1999)

[7] J.H. Lee, K.S. Cho, J. Lee, J. Yoo, J. Lee, J .Chung, Diptericin-like protein: an immune response gene regulated by the anti-bacterial gene induction pathway in Drosophila, Gene 271 (2001) 233-238

[8] Sanders CR, Prosser RS., Bicelles: a model membrane system for all seasons? Structure 6:12271234(1998)

[9] Jennifer A. Whiles, Raymond Deems, Regitze R. Vold, and Edward A. Dennis, Bicelles in structurefunction studies of membrane-associated proteins, Bioorganic Chemistry 30 (2002) 431442

[10] Jeremy N. S. Evans, Biomolecualar NMR Spectroscopy, Oxford University Press, 1995

[11] Waghu F.H., Gopi L., Barai R.S., Ramteke P., Nizami B., Idicula-Thomas, S. CAMP: Collection of sequence and structures of antimicrobial peptides. Nucleic Acids Res., 2014, 42, D1154-1158

[12] Yeaman M.R., Yount N.Y., Mechanism of antimicrobial peptides action and resistance. Pharmacol. Rev., 2003, 55, 27-55

[13] T.H. Lee, K.N. Hall, M.I. Aguilar, Antimicrobial peptide structure and mechanism of action: A focus on the role of membrane structure, Current topics in Medicinal Chemistry, 16, 25-39(2016)

[14] Cohen, M.L, Epidemiology of drug resistance: implications for a post-antimicrobial era. Science, 1992, 257, 1050-1055

[15] Wang G., Improved methods for classification, prediction and design of antmicrobial peptides. Methods Mol. Biol., 2015, 1268 43-66

[16] Cavanagh J., Fairbrother W.J., Palmer, A.G, Rance M., Skelton N.J, Protein NMR Spectroscopy: Principles and Practice, Elsevier P21 , 2007

[17] Kurt Wuethrich: NMR of Proteins and Nucleic Acids, Wiley 1986

[18] Ad Bax: Two-Dimensional NMR and Protein Structure, Annu. Rev. Biochem. 1989. 58:223-56

[19] NMR of Macromolecules - A practical approach, Oxford University Press 1993

[20] Atreya H.s., Principles and Applications of NMR Spectroscopy, Youtube, 28^{th} August 2016

[21] Atta ur Rahman, Nuclear magnetic resonance, Springer, 2008

[22] John Cavanagh, Nicholas J. Skelton, Wayne J. Fairbrother, Mark Rance, Arthur G. Palmer, III, Protein NMR Spectroscopy: Principles and Practice, Academic Press Inc, 1995

[23] Ailsa M. McManus, Laszlo Otvos, Jr., Ralf Hoffmann, and David J. Craik, Conformational Studies by NMR of the Antimicrobial Peptide, Drosocin, and Its Non-Glycosylated Derivative: Effects of Glycosylation on Solution Conformation, Biochemistry 1999, 38, 705-714

[24] Sparky Tutorial and Reference Manual 3.115

[25] E. Gonzalez, D. Dolino, D. Schwartzenburg, and M. A. Steiger, Dipeptide Structural Analysis Using Two-Dimensional NMR for the Undergraduate Advanced Laboratory, Journal of Chemical Education, 2014.

[26] Wishart, D. S., Sykes, B. D., and Richards, F. M. (1991) J. Mol. Biol. 222, 311-333.

[27] Wishart, D. S., Sykes, B. D., and Richards, F. M. (1992) Biochemistry 31, 1647-1651.

[28] Karplus M. Contact electronspin coupling of nuclear magnetic moments. J Chem Phys. 1959;30:1115.

[29] Bruce Coxon, Developments in the Karplus equation as they relate to the NMR coupling constants of carbohydrates, Adv Carbohydr Chem Biochem. 2009; 62: 1782.

[30] Dalton L. Karplus equation. Theoretical calculation links NMR coupling constant to molecular geometry. Chem Eng News. 2003;81:3739.